Applied Surface Science 353 (2015) 150–157

Contents lists available at ScienceDirect

Applied Surface Science

journal homepage: www.elsevier.com/locate/apsusc

The effect of anatase TiO_2 surface structure on the behavior of ethanol adsorption and its initial dissociation step: A DFT study

Riguang Zhang[a], Zhixue Liu[a], Lixia Ling[a,b], Baojun Wang[a,*]

[a] Key Laboratory of Coal Science and Technology of Ministry of Education and Shanxi Province, Taiyuan University of Technology, Taiyuan 030024, Shanxi, PR China

[b] Research Institute of Special Chemicals, Taiyuan University of Technology, Taiyuan 030024, Shanxi, PR China

ARTICLE INFO

Article history:
Received 6 February 2015
Received in revised form 9 June 2015
Accepted 13 June 2015
Available online 20 June 2015

Keywords:
Ethanol
Adsorption
Dissociation
Anatase surface
Density functional theory

ABSTRACT

The perfect and defective surfaces of anatase TiO_2 including (1 0 1) and (0 0 1) surfaces have been chosen to probe into the effect of anatase TiO_2 surface structure on the behavior of ethanol adsorption and initial dissociation step. Here, the results are obtained by density functional theory (DFT) calculation together with the periodic slab model. Our results show that the surface structure of anatase TiO_2 can obviously affect the behavior of ethanol adsorption and the catalytic activity of its initial dissociation step; firstly, on the perfect and defective surfaces of anatase (1 0 1), ethanol dominantly exists in the form of molecule adsorption; however, ethanol is the dissociative adsorption on the hydroxylated anatase (0 0 1), and the coexistences of molecular and dissociation adsorption modes on the perfect anatase (0 0 1). On the other hand, the initial dissociation step of ethanol with molecule adsorption prefers to begin with its O–H bond cleavage leading to CH_3CH_2O and H species rather than the cleavage of its α-C–H, β-C–H, C–C and C–O bonds, namely, the preferable O–H bond cleavage for the initial dissociation step of ethanol is independent of the surface structure of anatase TiO_2; however, the corresponding catalytic activity of ethanol initial dissociation step with the O–H bond cleavage on different anatase TiO_2 surfaces is in the following order: hydroxylated (0 0 1) > perfect (0 0 1) > defective (1 0 1) > perfect (1 0 1), suggesting that the catalytic activity for the initial dissociation step of ethanol is sensitive to the surface structure of anatase TiO_2, and the hydroxylated (0 0 1) is the most favorable surface. Among these surfaces, the most favorable product for the initial dissociation step of ethanol is CH_3CH_2O species.

1. Introduction

Ethanol, as an alternative fuel to produce hydrogen or as a feedstock for a possible green chemistry, has drawn much attention due to its unique advantages, such as high hydrogen content and non-toxicity [1–4]. Alternatively, ethanol can be used as carbon source in the synthesis of carbon nanotubes that have the outstanding physical and chemical properties [5,6]. In industry, ethanol dissociation is one of the key issues [7]. Recently, a large number of studies have revealed that ethanol conversion and hydrogen yield largely depend on catalysts and reaction conditions [8,9]. Thus, selecting a suitable and durable catalyst becomes a crucial issue in the entire process, which can determine the capability to selective cleavage of α-C–H, β-C–H, C–C or C–O bonds during ethanol dissociation [7,10], which leads to different products on the catalyst. Thus, the studies about ethanol's surface chemistry on the catalytically active surfaces become important [11–13].

In order to clarify ethanol's surface chemistry, especially the mechanism of ethanol adsorption and dissociation over the catalytically active surfaces, extensive studies have been carried out on the pure metal and compound of transition metal [3,7,14,15]. Zhang et al. [7] have investigated ethanol dissociation on Rh(2 1 1) surface by density functional theory (DFT) methods, indicating that ethanol proceeds directly to CH_3CHOH by the α-C–H bond scission. Williams et al. [3] have experimentally studied ethanol adsorption and dissociation on Pd(1 1 1), suggesting that ethanol dissociation proceeds directly to ethoxide (not hydroxyethyl). Choi and Liu [14] investigated ethanol dissociation on Rh(1 1 1), suggesting that the most favorable pathway is the O–H bond scission to CH_3CH_2O intermediate. Barthos et al. [16] researched ethanol dissociation over Mo_2C/carbon catalysts, suggesting that H_2 and acetaldehyde are the major products.

Alcohol chemistry on titanium dioxide (TiO_2) surfaces is a classic topic in both catalysis and surface science [17–22]. TiO_2-based has been widely applied as a photocatalyst to produce hydrogen from

* Corresponding author at: No. 79 Yingze West Street, Taiyuan 030024, PR China. Tel.: +86 351 6018239; fax: +86 351 6041237.
E-mail addresses: wangbaojun@tyut.edu.cn, quantumtyut@126.com (B. Wang).

http://dx.doi.org/10.1016/j.apsusc.2015.06.059
0169-4332/

ethanol in the last decades [2,23–28]. TiO_2 exists in the form of three polymorphs: rutile, anatase, and brookite; rutile and anatase TiO_2 materials have been widely used [20,29–31], moreover, the commercial TiO_2 powders often used as catalyst support are the mixtures of rutile and anatase [32]. Therefore, it is necessary to probe into ethanol adsorption and dissociation over different types of TiO_2, which will provide microscopic insight into the effect of TiO_2 surface structure on the behavior of ethanol adsorption and dissociation step [2].

For the rutile TiO_2, extensive studies often focus on the energetically preferred (1 1 0) as a model surface [2,17,18,33,34]. Guo et al. [18] have experimentally and theoretically investigated methanol dissociation on TiO_2(1 1 0), and found that the O–H bond cleavage is more favorable. Methanol dissociation at a bridging vacancy of rutile (1 1 0) was favored to give rise to a hydroxyl group at a bridging atom [33]. Ethanol dissociation at the oxygen vacancy of rutile occurs by the O–H bond cleavage to produce ethoxy [21,35–38]. Ma et al. [2] have experimentally and theoretically studied the photocatalytic dissociation of ethanol on the rutile (1 1 0), indicating that ethanol is molecular adsorption state, and the adsorbed ethanol can be converted to acetaldehyde via the O–H cleavage or the α-C–H breaking. Hansen et al. [39] have studied ethanol dissociation on the rutile (1 1 0) by high-resolution scanning tunneling microscopy (STM) measurements and DFT calculations, suggesting that molecularly and dissociatively adsorbed alcohol species co-exist on the regular surface Ti sites, meanwhile, the clear-cut assignment of $EtOH_{Ti}$ molecules, EtO_{Ti} and EtO_{br} ethoxides on rutile (1 1 0) are obtained. Martinez et al. [40] investigated ethanol dissociation on the defective rutile (1 1 0) surface, the three different EtOH-related species are known: molecularly and dissociatively adsorbed EtOH at the Ti_{5c} site ($EtOH_{Ti}$ and EtO_{Ti}, respectively) and ethoxides adsorbed at the O_{br} vacancy site (EtO_{br}); meanwhile, DFT calculation results show that oxygen vacancies are the reactive sites for ethanol dissociation via the O–H bond scission. Muir et al. [34] have theoretically studied the adsorption of C_2H_5OH, the co-adsorption of C_2H_5O and H species on the perfect and O-defected TiO_2(1 1 0) surfaces, suggesting that ethanol is molecular adsorption on both surfaces, and the O–H bond scission of ethanol should be exothermic reaction.

For the anatase TiO_2, the crystal facets dominantly include the thermodynamically stable (1 0 1) surface and the chemically more reactive (0 0 1) [41,42]. Meanwhile, the minority (0 0 1) surface played a key role in the reactivity of anatase nanoparticles [43,44], and is more reactive than the majority (1 0 1) surface; up to now, a large percent of (0 0 1) facets (as large as 47%) have been successfully synthesized in anatase TiO_2 crystal [44,45]. Photocatalysis of CH_3OH on the anatase (1 0 1) has shown that CH_3OH dominantly exists in the form of molecular adsorption with only very small amount of CH_3OH in the form of dissociative adsorption [20]. Han et al. [46] have investigated methanol adsorption, the co-adsorption of dissociation products via the individual O–H, C–O and C–H bond cleavage over the perfect and defective anatase TiO_2(1 0 1) surface, respectively, suggesting that on the perfect anatase (1 0 1), although methanol dissociation via the O–H scission is endothermic, it is the most favorable route compared with C–O and C–H bond scission in the view of thermodynamics; however, on the defective surface, methanol dissociation via the O–H scission is exothermic, which is also the most favorable route. Recently, only the studies by Nadeem et al. [47] have experimentally suggested that ethanol dissociation on the bare TiO_2 to yield surface ethoxide species. In addition, anatase (0 0 1) is very reactive toward water and methanol adsorption, (0 0 1) surface strongly favors the dissociation rather than the molecular adsorption on (1 0 1) surface [43].

On the basis of above reported studies, we can obtain that the adsorption and dissociation of methanol and ethanol on different types of TiO_2 is significant; up to now, for the rutile TiO_2, a large number of studies about the adsorption and dissociation of methanol and ethanol have been investigated; however, to the best of our knowledge, few studies about the adsorption and dissociation of ethanol on different anatase TiO_2 surfaces, as well as the effect of anatase TiO_2 surface structure on the adsorption and dissociation behavior of ethanol, have been reported at the molecular level; as a result, it is still unclear: (1) is ethanol molecular adsorption or dissociative adsorption on different anatase TiO_2 surfaces? (2) Between the perfect and defective surfaces of anatase TiO_2, which is more favorable for the adsorption and dissociation of ethanol? (3) What is the preferable cleavage bond of ethanol initial dissociation step? (4) Among anatase TiO_2 surfaces, which is the most favorable surface for the initial dissociation step of ethanol?

In this study, in order to tackle above these puzzles, the perfect and defective surfaces of anatase TiO_2 including (1 0 1) and (0 0 1) surfaces have been chosen to probe into the effect of anatase TiO_2 surface structure on the adsorption and dissociation behavior of ethanol. Here, the results are obtained by density functional theory (DFT) calculation together with the periodic slab model. We expected to obtain a clear picture for the adsorption and the initial dissociation step of ethanol on different anatase TiO_2 surfaces, which may provide useful information for the rational design of better catalyst in ethanol dissociation.

2. Computational details

2.1. Different anatase TiO_2 surfaces

2.1.1. (a) Anatase (1 0 1) surface

The perfect anatase (1 0 1) surface has the highly corrugated form, as shown in Fig. 1(a). It contains both five-fold and six-fold surface Ti atoms (Ti_{5c} and Ti_{6c}), as well as two types of surface O atoms referred to as the bridging (O_{2c}) and in-plane oxygen (O_{3c}). The defective anatase (1 0 1) surface is modeled by removing a surface bridging oxygen atom from the outermost layer [22,32], as shown in Fig. 1(b).

A 12 layers slab with a $p(1 \times 3)$ unit cell and the vacuum space of 10 Å is used to model the anatase (1 0 1) surface, and the bottom six-atom-layers are constrained at the bulk position, whereas the upper six-atom-layers together with the adsorbed species are allowed to relax. Han et al. [46] have investigated Pt clusters adsorption and growth on the same $p(1 \times 3)$ model.

2.1.2. (b) Anatase (0 0 1) surface

The perfect anatase (0 0 1) surface has also the corrugated form, as shown in Fig. 2(a). It only contains Ti_{5c}, and two types of surface O atoms: O_{2c} and O_{3c}, as well as the Hole site. For anatase, the most available anatase crystals are dominated by the thermodynamically stable (1 0 1) facets rather than the more reactive (0 0 1) facets [44,45,48]; however, a large percent of (0 0 1) facets (as large as 47%) have been successfully synthesized in anatase crystals [44]. Meanwhile, Gong et al. [43] have investigated the effect of hydration on formic acid adsorption, suggesting that the dissociative adsorption of H_2O on the anatase (0 0 1)-(1×1) surface significantly decreases the surface energy of anatase (0 0 1) from 0.98 J m^{-2} of the clean surface to 0.57 and 0.33 J m^{-2} with water coverage between 1/3 and 1/2 ML, respectively, subsequently, the stiff O_{2c}–Ti_{5c}–O_{2c}–Ti_{5c} framework can be formed, which can form the tighter bonds with O_{2c}, in this way, O_{2c} is indirectly stabilized. As a result, the OH groups formed on the anatase (0 0 1) surface can strongly affect the stabilities of anatase (0 0 1) surface [49]. Therefore, the defective anatase (0 0 1) surface is modeled by the partial hydroxylation with OH groups at Ti_{5c} atoms in this study, as shown in Fig. 2(b).

A 12 layers slab with a $p(3 \times 2)$ unit cell and the vacuum space of 10 Å is used to model anatase (0 0 1) surface. The bottom

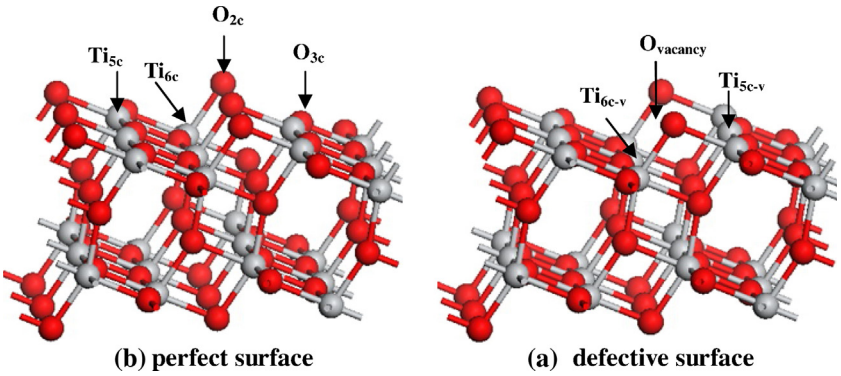

Fig. 1. The surface morphology of (a) perfect and (b) defective anatase (1 0 1) surfaces. Ti_{5c} and Ti_{6c} refer to five-fold and six-fold surface Ti atoms, respectively; O_{2c} and O_{3c} refer to the bridging and in-plane oxygen atoms, respectively. The red and grey balls denote O and Ti atoms, respectively. (For interpretation of the references to color in this figure legend, the reader is referred to the web version of the article.)

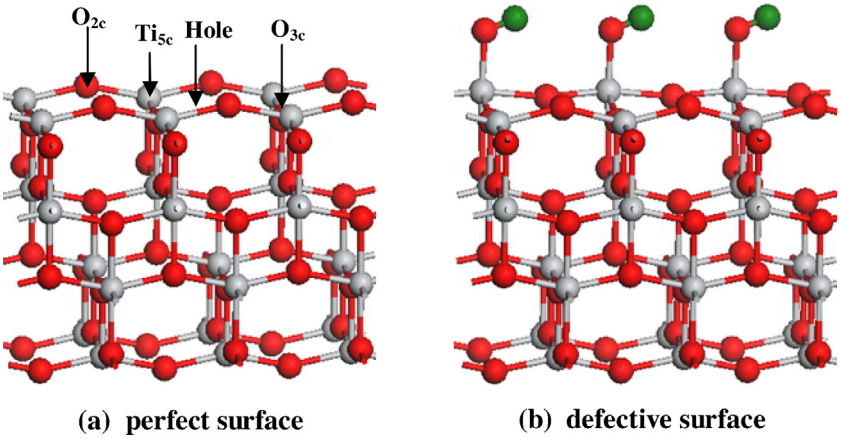

Fig. 2. The surface morphology of (a) perfect and (b) defective anatase (0 0 1) surfaces. See Fig. 1 for color coding. In addition, the green balls represent the surface hydroxylated H atoms.

six-atom-layers are constrained at the bulk position, whereas the upper six-atom-layers together with the adsorbed species are allowed to relax. The defective anatase (0 0 1) surface is modeled with three OH groups at the three Ti_{5c} atoms.

2.2. Calculations methods

All calculations have been carried out in the framework of DFT using $Dmol^3$ program package in Materials Studio 5.5 [50,51], the main calculations here are conducted with the generalized gradient approximation with the Perdew–Wang exchange–correlation functional (GGA-PW91) [52,53]. In the computation, the spin-unrestricted (spin-polarized) [46,54] is included in the relaxation of all the structures presented in our study. The inner electrons of metal atoms are kept frozen, and replaced by an effective core potential (ECP) [55,56], and other atoms are treated with an all-electron basis set. The double-numeric quality basis set with polarization functions (DNP) is used [57]. Brillouin-zone integrations have been performed using $1 \times 2 \times 1$ Monkhorst-Pack grid and a Methfessel-Paxton smearing of 0.005 Ha. On the other hand, in order to determine the accurate activation barriers of the reactions, complete LST/QST approach is chosen to search for transition states [58]. In addition, frequency analysis has been used to validate the transition state, TS confirmation is performed on every transition state to confirm that they lead to the desired reactants and products.

About the adsorption of various reactants, intermediates, and products on anatase TiO_2 surface, the adsorption energy is defined as $E_{ads} = E_{slab} + E_{adsorbate} - E_{adsorbate/slab}$, where the $E_{adsorbate/slab}$ is the total energy of anatase TiO_2 surface with the adsorbate; E_{slab} is the energy of the pure anatase TiO_2 surface; and $E_{adsorbate}$ is the energy of the gas-phase adsorbate. By definition, a negative value corresponds to exothermic adsorption.

For a reaction such as $AB \rightarrow A + B$ on anatase TiO_2 surface, the reaction energy (ΔH) and activation barrier (E_a) are calculated according to the following formulas:

$$\Delta H = E_{(A+B)/TiO_2} - E_{AB/TiO_2}$$

$$E_a = E_{TS/TiO_2} - E_{AB/TiO_2}$$

where $E_{(A+B)/TiO_2}$ – the total energy for the co-adsorbed A and B on anatase TiO_2 surface; E_{AB/TiO_2} – the total energy for the adsorbed AB on anatase TiO_2 surface; E_{TS/TiO_2} – the total energy of transition state for the reaction $AB \rightarrow A + B$.

3. Results and discussion

In this section, the adsorptions of reactants and all possible intermediates involved in the initial dissociation step of ethanol are firstly investigated on different anatase TiO_2 surfaces; then, the mechanism for the initial dissociation step of C_2H_5OH is systematically discussed; further, the differences of ethanol dissociation among these surfaces of anataseTiO_2 are identified.

For the initial dissociation step of ethanol, five possible reactions (R1)–(R5) have been examined, which are the initial dissociation

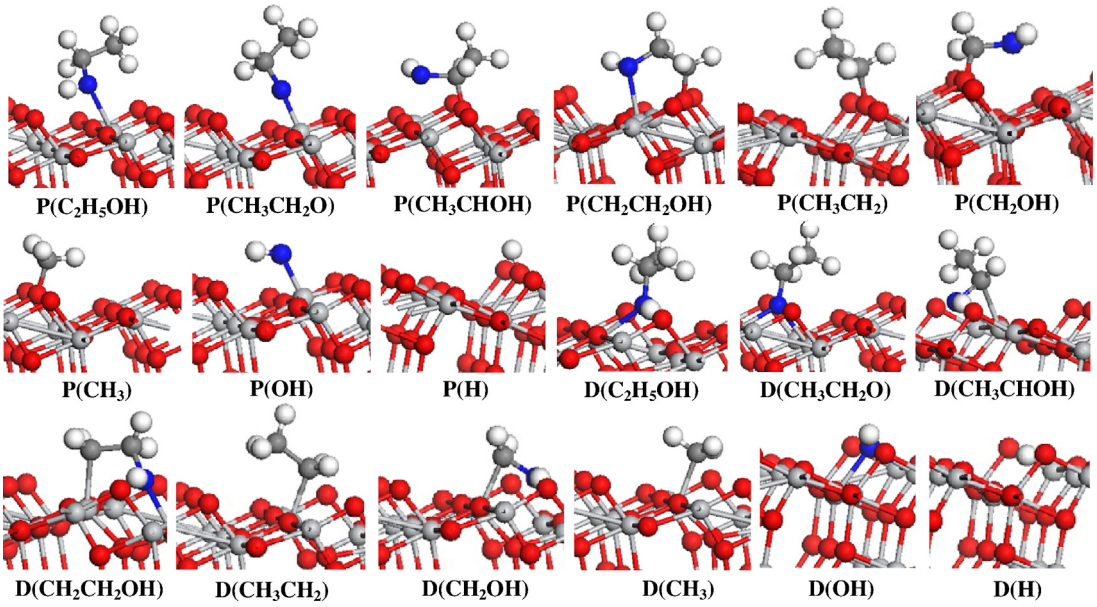

Fig. 3. The most stable adsorption configurations of reactants and all possible intermediates involved in the initial dissociation step of ethanol on the perfect and defective anatase (1 0 1) surfaces. Ti, C, H, O atoms and O atom of ethanol are shown in the light grey, grey, white, red and blue balls, respectively. (For interpretation of the references to color in this figure legend, the reader is referred to the web version of the article.)

of ethanol with its cleavage of O–H, α-C–H, β-C–H, C–C and C–O bonds, respectively.

$$C_2H_5OH \rightarrow CH_3CH_2O + H \quad (R1)$$

$$C_2H_5OH \rightarrow CH_3CHOH + H \quad (R2)$$

$$C_2H_5OH \rightarrow CH_2CH_2OH + H \quad (R3)$$

$$C_2H_5OH \rightarrow CH_3 + CH_2OH \quad (R4)$$

$$C_2H_5OH \rightarrow CH_3CH_2 + OH \quad (R5)$$

3.1. Anatase (1 0 1) surfaces

On the anatase (1 0 1) surface, the most stable configurations of the related species involved in the initial dissociation step of ethanol are shown in Fig. 3. The adsorption energies and key geometrical parameters are listed in Table 1.

Our results show that on the perfect surface, ethanol dominantly adsorbs at the Ti_{5c} site, other related species mainly adsorb at the Ti_{5c} and/or O_{2c} sites; however, on the defective surface, ethanol dominantly adsorbs at the O-vacancy site, other related species prefer to adsorb at the O-vacancy sites and the adjacent lower coordination Ti atoms, indicating that O-vacancy becomes the favorable adsorption site instead of O_{2c} site on the perfect surface. Meanwhile, the adsorption energies of all related species on the defective surface are stronger than those on the perfect surface; ethanol exists in the form of molecular adsorption on both surfaces.

Fig. 4(a) displays the potential energy profile for the initial dissociation step of ethanol together with the structures of transition states and final states on the perfect anatase (1 0 1) surface. Our results show that among five pathways, the pathway (R1) with the O–H bond scission of C_2H_5OH to CH_3CH_2O and H species via P(TS1) is the most favorable both thermodynamically and kinetically, which only needs to overcome an activation barrier of 92.1 kJ mol^{-1} with the reaction energy of −2.6 kJ mol^{-1}; in P(TS1),

Table 1
The adsorption energy (kJ mol^{-1}) and key geometrical parameters (Å) of reactants and all possible intermediates involved in the initial step of ethanol dissociation on the perfect and defective anatase (1 0 1) surfaces.

Surface	Species	E_{ads}	Configuration	Key parameters
Perfect	C_2H_5OH	111.1	Atop on Ti_{5c} via O	O–Ti_{5c}: 2.239
	CH_3CH_2O	111.9	Atop on Ti_{5c} via O	O–Ti_{5c}: 1.847
	CH_3CHOH	227.0	Atop on O_{2c} via α-C	α-C–O_{2c}: 1.392
	CH_2CH_2OH	265.9	Bridge via β-C at O_{2c} and O at Ti_{5c}	β-C–O_{2c}: 1.420, O–Ti_{5c}: 2.256
	CH_3CH_2	228.7	Atop on O_{2c} via α-C	α-C–O_{2c}: 1.442
	CH_2OH	201.0	Atop on O_{2c} via C	C–O_{2c}: 1.441, O–Ti_{5c}: 2.235
	CH_3	191.5	Atop on O_{2c} via C	C–O_{2c}: 1.431
	OH	157.2	Atop on Ti_{5c} via O	O–Ti_{5c}: 1.826
	H	278.5	Atop on O_{2c}	H–O_{2c}: 0.967
Defective	C_2H_5OH	169.5	Atop on $Ti_{5c\text{-}v}$ via O	O–Ti_{5c}: 2.256
	CH_3CH_2O	418.5	Atop on vacancy via O	O–Ti_{5c}: 1.957, 2.152
	CH_3CHOH	271.2	Atop on Ti_{5c} via α-C and O	α-C–Ti_{5c}: 2.101, O–Ti_{5c}: 2.292
	CH_2CH_2OH	306.5	Bridge via β-C on $Ti_{5c\text{-}v}$ and O on $Ti_{6c\text{-}v}$	β-C–Ti_{5c}: 2.155, O–Ti_{5c}: 2.286
	CH_3CH_2	262.6	Atop on $Ti_{5c\text{-}v}$ via α-C	α-C–$Ti_{5c\text{-}v}$: 2.081
	CH_2OH	271.5	Atop on $Ti_{5c\text{-}v}$ via C	C–$Ti_{5c\text{-}v}$: 2.092
	CH_3	293.5	Atop on $Ti_{5c\text{-}v}$ via C	C–Ti_{5c}: 2.083
	OH	478.8	Atop on vacancy via O	O–$Ti_{5c\text{-}v}$: 2.008, O–$Ti_{6c\text{-}v}$: 2.141
	H	260.5	Atop on vacancy	H–$Ti_{5c\text{-}v}$: 1.956, H–$Ti_{6c\text{-}v}$: 1.921

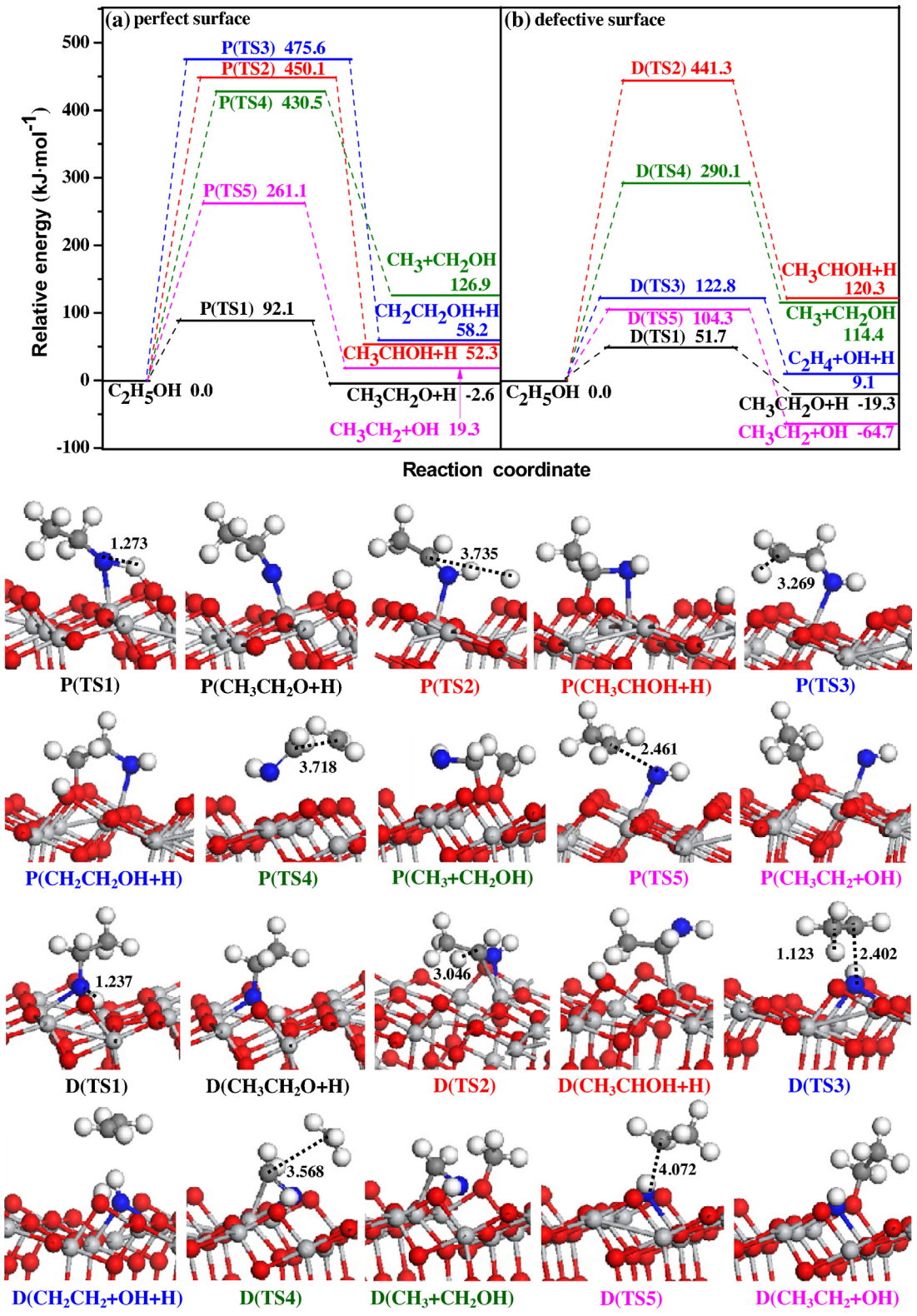

Fig. 4. The potential energy profile for the initial dissociation step of ethanol on the (a) perfect and (b) defective anatase (1 0 1) surfaces. See Fig. 3 for color coding. Bond lengths are in Å.

the distances between O and H atoms is elongated to 1.273 Å from 0.973 Å in C_2H_5OH. The pathway (R2) with the α-C–H bond scission of C_2H_5OH produces CH_3CHOH and H species via P(TS2), in P(TS2), the distances between α-C and H atoms is elongated to 3.735 Å from 1.098 Å in C_2H_5OH. The pathway (R3) with the β-C-H bond scission of C_2H_5OH leads to CH_2CH_2OH and H species via P(TS3), in P(TS3), the distances between β-C and H atoms is elongated to 3.269 Å from 1.097 Å in C_2H_5OH. The pathway (R4) with the C–C bond cleavage of C_2H_5OH results in CH_3 and CH_2OH species via P(TS4), in P(TS4), the distance between α-C and β-C is elongated to 3.718 Å from 1.511 Å in C_2H_5OH. The pathway (R5) with the C–O bond cleavage of C_2H_5OH leads to CH_3CH_2 and OH species via P(TS5), in P(TS5), the

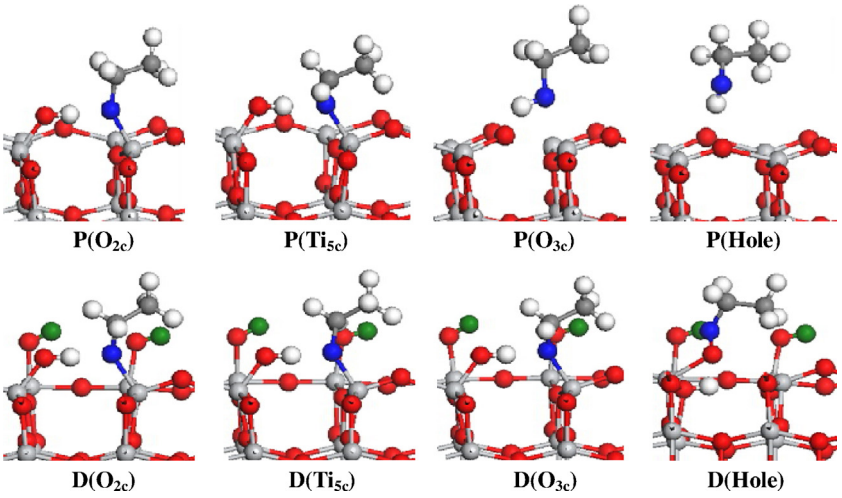

Fig. 5. The adsorption configuration of C_2H_5OH at different adsorption sites on the perfect and hydroxylated anatase (0 0 1) surfaces. See Figs. 2 and 3 for color coding.

distances between α-C and O atoms is elongated to 2.461 Å from 1.465 Å in C_2H_5OH.

Similarly, as shown in Fig. 4(b) on the defective anatase (1 0 1) surface, our results show that among five pathways, the pathway (R1) with C_2H_5OH dissociation into CH_3CH_2O and H species via D(TS1) is the most favorable kinetically, this pathway has an activation barrier of 51.7 kJ mol^{-1}, and it is exothermic by 19.3 kJ mol^{-1}; in D(TS1), the distances between O and H atoms is elongated to 1.237 Å from 0.984 Å in C_2H_5OH. For (R2), C_2H_5OH dissociates into CH_3CHOH and H species via D(TS2), in D(TS2), the distances between α-C and H atoms is elongated to 3.046 Å from 1.095 Å in C_2H_5OH. The pathway (R3) is the β-C–H bond cleavage of C_2H_5OH, however, our results show that during this process, the α-C–O bond cleavage of C_2H_5OH firstly produces C_2H_4 species via D(TS3) instead of CH_2CH_2OH formation by the β-C–H bond cleavage of C_2H_5OH, this elementary reaction has an activation barrier of 122.8 kJ mol^{-1}, and it is endothermic by 9.1 kJ mol^{-1}; in D(TS3), the distances between C and O atoms is elongated to 2.402 Å from 1.488 Å in C_2H_5OH, and the distances between β-C and H atoms is elongated to 1.123 Å from 1.098 Å in C_2H_5OH. For (R4), the C–C bond cleavage of C_2H_5OH leads to CH_3 and CH_2OH species through D(TS4), in D(TS4), the distances between α-C and β-C atoms is elongated to 3.568 Å from 1.508 Å in C_2H_5OH. For (R5), the α-C–O bond cleavage of C_2H_5OH via D(TS5) can form CH_3CH_2 and OH species, in D(TS5), the distances between α-C and O atoms is elongated to 4.072 Å from 1.485 Å in C_2H_5OH.

As shown in Fig. 4, among five pathways for the initial dissociation step of ethanol, C_2H_5OH dissociation into CH_3CH_2O and H species via the O–H bond scission is the most favorable pathway on the anatase (1 0 1) surface; on the perfect surface, this elementary reaction has the corresponding activation barrier and reaction energy of 92.1 and −2.6 kJ mol^{-1}, respectively; whereas, the activation barrier and reaction energy on the defective surface are 51.7 and −19.3 kJ mol^{-1}, respectively; these results suggest that the most favorable pathway for the initial dissociation step of ethanol on the defective (1 0 1) is more favorable than that on the perfect (1 0 1). Further, the same bond cleavage involving in the initial dissociation step of ethanol is more favorable on the defective (1 0 1) surface than that on the prefect (1 0 1) surface. In addition, Han et al. [46] have compared the adsorption and dissociation of CH_3OH on the anatase (1 0 1) surface, suggesting that the defective anatase (1 0 1) surface is more favorable than the perfect one for CH_3OH dissociation.

On the defective surface, the O-vacancy sites and its adjacent lower coordinate Ti sites are the active sites for the related species adsorption, the presence of O-vacancy results in the increase of the adsorption active sites consisted of O-vacancy sites and its adjacent lower coordinate Ti sites, as a result, the numbers of active sites increase, which make the initial dissociation step of ethanol become more favorable under the realistic condition.

3.2. Anatase (0 0 1) surfaces

On the perfect surface, ethanol adsorption at the O_{2c}, O_{3c}, Ti_{5c} and Hole sites have been examined. Among these sites, the molecular and dissociative adsorptions co-exist, as shown in Fig. 5. When C_2H_5OH adsorbs at the O_{2c} and Ti_{5c} sites, respectively, both are the dissociative adsorption to produce CH_3CH_2O adsorbed at the Ti_{5c} site via O atom and H located at the O_{2c} site to form the hydroxylated group. However, C_2H_5OH adsorbs at the O_{3c} and Hole sites via O atom, C_2H_5OH is the molecular adsorption mode with the corresponding adsorption energies of 128.5 and 102.3 kJ mol^{-1}, respectively, suggesting that C_2H_5OH adsorbed at the O_{3c} site is more stable than that adsorbed at the Hole site.

On the hydroxylated anatase (0 0 1), as shown in Fig. 5, ethanol adsorption at different sites are all the dissociative adsorption leading to CH_3CH_2O and H species, namely, ethanol is the dissociative adsorption on the hydroxylated anatase (0 0 1).

Above results show that on the perfect and hydroxylated anatase (0 0 1) surfaces, C_2H_5OH dominantly exists in the form of the dissociative adsorption, which is dominantly responsible for the initial dissociation step of C_2H_5OH leading to CH_3CH_2O and H species. In addition, previous studies have shown that OH groups on the hydroxylated anatase (0 0 1) surface can strongly affect the initial adsorption of the compound on the surface [49].

In addition, as mentioned above, since the dissociative adsorption of H_2O on the anatase (0 0 1) is supported by many previous works, in this study, the defective anatase (0 0 1) surface is modeled by the partial hydroxylation. Moreover, the present results show that on the anatase (0 0 1) perfect surface, ethanol with the molecular and dissociative adsorptions co-exist, in which the dissociative adsorption of ethanol can produce H and CH_3CH_2O species; subsequently, the formed H atom prefers to be adsorbed at O_{2c} site, which makes the Ti–O bond cleavage of the anatase (0 0 1) perfect surface, as a result, Ti is changed to Ti^{3+} from Ti^{4+}. Further, a recent experimental work [59] has raised a different point, which have

claimed that water adsorption is not active at room temperature, but can be activated for Ti^{3+} point defects at the ridge. Therefore, the formed Ti^{3+} from the Ti–O bond cleavage of the anatase (0 0 1) perfect surface is also beneficial to H_2O dissociation and further formation of the hydroxylated anatase (0 0 1) surface, this is the reason why the anatase (0 0 1) defective surface is modeled by the partial hydroxylation in this study.

3.3. General discussion

Firstly, for the effect of anatase TiO_2 surface structures on the adsorption behavior of ethanol, our results show that on the perfect and defective surfaces of anatase (1 0 1), ethanol dominantly exists in the form of the molecular adsorption, C_2H_5OH prefers to adsorb at the Ti_{5c} site via O atom, while it prefers to adsorb at the O-vacancy via O atom on the defective anatase (1 0 1); moreover, on the defective surface, the O-vacancy and its adjacent lower coordinated Ti site become the most favorable adsorption site instead of O_{2c} site for other related species. On the other hand, on the anatase (0 0 1) surface, ethanol is the coexistence of molecular and dissociative adsorption modes on the perfect surface, in which C_2H_5OH adsorbed at the O_{3c} and Hole sites via O atom is the molecular adsorption mode, and C_2H_5OH at the O_{3c} site is more stable than that at the Hole site; on the hydroxylated surface, ethanol is the dissociative adsorption leading to CH_3CH_2O and H species.

Secondly, for the effect of anatase TiO_2 surface structures on the initial dissociation step of ethanol, our results show that among five reactions with its cleavage of O–H, α-C–H, β-C–H, C–C and C–O bonds of ethanol, the most favorable pathway for the initial step of ethanol dissociation is carried out by the O–H bond cleavage leading to CH_3CH_2O and H species.

On the anatase (1 0 1) surface, the activation barrier and reaction energy are 92.1 and $-2.6\,kJ\,mol^{-1}$ on the perfect surface, respectively, whereas, both are 51.7 and $-19.3\,kJ\,mol^{-1}$ on the defective surface, respectively; namely, the initial dissociation step of ethanol on the defective surface via the O–H bond cleavage is more favorable than that on the perfect one; the cause may be that O-vacancy site and its adjacent lower coordinated Ti site become the main active site on the defective anatase (1 0 1), the presence of O-vacancy increase the number of active sites, thus, ethanol dissociation on the defective surface is more favorable than that on the perfect surface under the realistic condition.

On the anatase (0 0 1) surface, the molecular adsorption and dissociative adsorption co-exist on the perfect surface; however, on the hydroxylated surface, all adsorption of ethanol at the different sites are all the dissociative adsorption, indicating that ethanol adsorption on the anatase (0 0 1) surface dominantly exists in the form of dissociative adsorption.

Finally, on the basis of above analysis, we can obtain that ethanol has the different existence forms on different anatase TiO_2 surfaces, which is dependent of anatase TiO_2 surface structure. Meanwhile, the preferable bond cleavage for the initial dissociation step of ethanol is independent of the surface structure of anatase TiO_2, the O–H bond cleavage is the most favorable; however, the catalytic activity for the initial dissociation step of ethanol is sensitive to anatase TiO_2 surface structure, the catalytic activity is as follows: hydroxylated (0 0 1) > perfect (0 0 1) > defective (1 0 1) > perfect (1 0 1), as a result, the hydroxylated anatase (0 0 1) is the most favorable surface for the initial dissociation step of ethanol. Namely, the hydroxylated anatase (0 0 1) is a promising candidate for an improved catalyst of ethanol dissociation. More importantly, the understanding about the effect of anatase TiO_2 surface structure on the catalytic activity of ethanol dissociation at the atomic level, which can potentially be applied to develop and design the more superior TiO_2-based catalysts, this is beyond the scope of the present study, which will be discussed in our next work.

4. Conclusions

In this work, the perfect and defective surfaces of anatase TiO_2 including (1 0 1) and (0 0 1) surfaces have been employed to investigate the effect of surface structure on the ethanol adsorption and its initial dissociation step by using density functional theory (DFT) method together with the periodic slab model. Our results show that ethanol is the molecular adsorption on the perfect and defective surfaces of anatase (1 0 1); however, ethanol dominantly exists in the form of dissociative adsorption on the anatase (0 0 1) surface; on the other hand, ethanol with molecular adsorption prefers to dissociate its O–H bond leading to CH_3CH_2O and H species rather than the cleavage of its α-C–H, β-C–H, C–C and C–O bonds; on the anatase (1 0 1) surface, the initial dissociation step of ethanol on the defective surface is more favorable than that on the perfect one. Among all these surfaces, the most favorable product for the initial dissociation step of ethanol is CH_3CH_2O species, the hydroxylated anatase (0 0 1) surface is the most favorable surface.

Acknowledgments

This work is financially supported by the National Natural Science Foundation of China (No. 21276003, 21476155 and 21276171), the Natural Science Foundation of Shanxi Province (No. 2014011012-2), the State Key Laboratory of Fine Chemicals (KF1205), the Program for the Top Young Academic Leaders of Higher Learning Institutions of Shanxi, and the Top Young Innovative Talents of Shanxi.

References

[1] A.V. Puga, A. Forneli, H. García, A. Corma, Production of H_2 by ethanol photoreforming on Au/TiO_2, Adv. Funct. Mater. 24 (2014) 241–248.
[2] Z.B. Ma, Q. Guo, X.C. Mao, Z.F. Ren, X. Wang, C.B. Xu, W.S. Yang, D.X. Dai, C.Y. Zhou, H.J. Fan, X.M. Yang, Photocatalytic dissociation of ethanol on TiO_2(110) by near-band-gap excitation, J. Phys. Chem. C 117 (2013) 10336–10344.
[3] R.M. Williams, S.H. Pang, J. Will Medlin, O-H versus C-H bond scission sequence in ethanol decomposition on Pd(111), Surf. Sci. 619 (2014) 114–118.
[4] M. Jiménez, R. Rincón, A. Marinas, M.D. Calzada, Hydrogen production from ethanol decomposition by a microwave plasma: Influence of the plasma gas flow, Int. J. Hydrogen Energy 38 (2013) 8708–8719.
[5] G. de Souza, N.M. Balzaretti, N.R. Marcílio, O.W. Perez-Lopez, Decomposition of ethanol over Ni-Al catalysts: effect of copper addition, Procedia Eng. 42 (2012) 335–345.
[6] J.X. Diao, H. Wang, W.L. Li, G. Wang, Z.Y. Ren, J.B. Bai, Effect of C-supported Co satalyst on the ethanol decomposition to produce hydrogen and multi-walled carbon nanotubes, Physica E 42 (2010) 2280–2284.
[7] J. Zhang, X.M. Cao, P. Hu, Z.Y. Zhong, A. Borgna, P. Wu, Density functional theory studies of ethanol decomposition on Rh(211), J. Phys. Chem. C 115 (2011) 22429–22437.
[8] M. Ni, D.Y.C. Leung, M.K.H. Leung, A review on reforming bio-ethanol for hydrogen production, Int. J. Hydrogen Energy 32 (2007) 3238–3247.
[9] A. Haryanto, S. Fernando, N. Murali, S. Adhikari, Current status of hydrogen production techniques by steam reforming of ethanol: a review, Energy Fuels 19 (2005) 2098–2106.
[10] R. Alcalá, M. Mavrikakis, J.A. Dumesic, DFT studies for cleavage of C-C and C-O bonds in surface species derived from ethanol on Pt(111), J. Catal. 218 (2003) 178–190.
[11] S.K. Xing, G.C. Wang, Reaction mechanism of ethanol decomposition on Mo_2C(100) investigated by the first principles study, J. Mol. Catal. A: Chem. 377 (2013) 180–189.
[12] D.C. Papageorgopoulos, Q. Ge, D.A. King, Synchronous thermal desorption and decomposition of ethanol on Rh{111}, J. Phys. Chem. C 99 (1995) 17645–17649.
[13] M. Li, W.Y. Guo, R.B. Jiang, L.M. Zhao, H.H. Shan, Decomposition of ethanol on Pd(111): A density functional theory study, Langmuir 26 (2010) 1879–1888.
[14] Y.M. Choi, P. Liu, Understanding of ethanol decomposition on Rh(111) from density functional theory and kinetic monte carlo simulations, Catal. Today 165 (2011) 64–70.
[15] D.Z. Mezalira, L.D. Probst, S. Pronier, Y. Batonneau, C. Batiot-Dupeyrat, Decomposition of ethanol over Ni/Al_2O_3 catalysts to produce hydrogen and carbon nanostructured materials, J. Mol. Catal. A: Chem. 340 (2011) 15–23.

[16] R. Barthos, A. Széchenyi, Á. Koós, F. Solymosi, The decomposition of ethanol over Mo_2C/carbon catalysts, Appl. Catal. A: Gen. 327 (2007) 95–105.
[17] R. Sánchez de Armas, J. Oviedo, M.A. San Miguel, J.F. Sanz, Methanol adsorption and dissociation on TiO_2(110) from first principles calculations, J. Phys. Chem. C 111 (2007) 10023–10028.
[18] Q. Guo, C.B. Xu, Z.F. Ren, W.S. Yang, Z.B. Ma, D.X. Dai, H.J. Fan, T.K. Minton, X.M. Yang, Stepwise photocatalytic dissociation of methanol and water on TiO_2(110), J. Am. Chem. Soc. 134 (2012) 13366–13373.
[19] C.B. Xu, W.S. Yang, Q. Guo, D.X. Dai, M.D. Chen, X.M. Yang, Molecular hydrogen formation from photocatalysis of methanol on TiO_2(110), J. Am. Chem. Soc. 135 (2013) 10206–10209.
[20] C.B. Xu, W.S. Yang, Q. Guo, D.X. Dai, M.D. Chen, X.M. Yang, Molecular hydrogen formation from photocatalysis of methanol on anatase-TiO_2(101), J. Am. Chem. Soc. 136 (2014) 602–605.
[21] Y.K. Kim, C.C. Hwang, Photoemission study on the adsorption of ethanol on clean and oxidized rutile TiO_2 (110)-1 × 1 surfaces, Surf. Sci. 605 (2011) 2082–2086.
[22] A. Tilocca, A. Selloni, Methanol adsorption and reactivity on clean and hydroxylated anatase(101) surfaces, J. Phys. Chem. B 108 (2004) 19314–19319.
[23] G.R. Bamwenda, S. Tsubota, T. Nakamura, M. Haruta, Photoassisted hydrogen production from a water-ethanol solution: a comparison of activities of Au-TiO_2 and Pt-TiO_2, J. Photochem. Photobiol. A: Chem. 89 (1995) 177–189.
[24] H. Idriss, E.G. Seebauer, Reactions of ethanol over metal oxides, J. Mol. Catal. A: Chem. 152 (2000) 201–212.
[25] J. Llorca, N. Homs, J. Sales, P.R. de la Piscina, Efficient production of hydrogen over supported cobalt catalysts from ethanol steam reforming, J. Catal. 209 (2002) 306–317.
[26] N. Strataki, M. Antoniadou, V. Dracopoulos, P. Lianos, Visible-light photocatalytic hydrogen production from ethanol-water mixtures using a Pt-CdS-TiO_2 photocatalyst, Catal. Today 151 (2010) 53–57.
[27] M. Murdoch, G.I.N. Waterhouse, M.A. Nadeem, J.B. Metson, M.A. Keane, R.F. Howe, J. Llorca, H. Idriss, The effect of gold loading and particle size on photocatalytic hydrogen production from ethanol over Au/TiO_2 nanoparticles, Nat. Chem. 3 (2011) 489–492.
[28] M.A. Nadeem, M. Murdoch, G.I.N. Waterhouse, J.B. Metson, M.A. Keane, J. Llorca, H. Idriss, Photoreaction of ethanol on Au/TiO_2 anatase: comparing the micro to nanoparticle size activities of the support for hydrogen production, J. Photochem. Photobiol. A: Chem. 216 (2010) 250–255.
[29] V.E. Henrich, G. Dresselhaus, H.J. Zeiger, Observation of two-dimensional phases associated with defect states on the surface of TiO_2, Phys. Rev. Lett. 36 (1976) 1335–1339.
[30] W.J. Lo, Y.W. Chung, G.A. Somorjai, Electron spectroscopy studies of the chemisorptions of O_2, H_2 and H_2O on the TiO_2(110) surfaces with varied stoichiometry: evidence for the photogeneration of Ti^{+3} and for its importance in chemisorptions, Surf. Sci. 71 (1978) 199–219.
[31] J. Schwitzgebel, J.G. Ekerdt, H. Gerischer, A. Heller, Role of the oxygen molecule and of the photogenerated electron in TiO_2-photocatalyzed air oxidation reactions, J. Phys. Chem. 99 (1995) 5633–5638.
[32] Y. Han, C.J. Liu, Q.F. Ge, Effect of surface oxygen vacancy on Pt cluster adsorption and growth on the defective anatase TiO_2(101) surface, J. Phys. Chem. C 111 (2007) 16397–16404.
[33] J. Oviedo, R. Sánchez-de-Armas, M.Á. San Miguel, J.F. Sanz, Methanol and water dissociation on TiO_2 (110): the role of surface oxygen, J. Phys. Chem. C 112 (2008) 17737–17740.
[34] J.N. Muir, Y. Choi, H. Idriss, Computational study of ethanol adsorption and reaction over rutile TiO_2 (110) surfaces, Phys. Chem. Chem. Phys. 14 (2012) 11910–11919.
[35] Z.R. Zhang, O. Bondarchuk, B.D. Kay, J.M. White, Z. Dohnálek, Direct visualization of 2-butanol adsorption and dissociation on TiO_2 (110), J. Phys. Chem. C 111 (2007) 3021–3027.
[36] L. Gamble, L.S. Jung, C.T. Campbell, Decomposition and protonation of surface ethoxys on TiO_2(110), Surf. Sci. 348 (1996) 1–16.
[37] Y.K. Kim, B.D. Kay, J.M. White, Z. Dohnálek, 2-propanol dehydration on TiO_2(110): The effect of bridge-bonded oxygen vacancy blocking, Surf. Sci. 602 (2008) 511–516.
[38] Y.K. Kim, B.D. Kay, J.M. White, Z. Dohnálek, Alcohol chemistry on rutile TiO_2(110): the influence of alkyl substituents on reactivity and selectivity, J. Phys. Chem. C 111 (2007) 18236–18242.
[39] J.Ø. Hansen, P. Huo, U. Martinez, E. Lira, Y.Y. Wei, R. Streber, E. Lægsgaard, B. Hammer, S. Wendt, F. Bescenbacher, Direct evidence for ethanol dissociation on rutile TiO_2(110), Phys. Rev. Lett. 107 (2011) 136102-1–136102-4.
[40] U. Martinez, J.Ø. Hansen, E. Lira, H.H. Kristoffersen, P. Huo, R. Bechstein, E. Lægsgaard, F. Besenbacher, B. Hammer, S. Wendt, Reduced step edges on rutile TiO_2(110) as competing defects to oxygen vacancies on the terraces and reactive sites for ethanol dissociation, Phys. Rev. Lett. 109 (2012) 155501-1–155501-5.
[41] M. Lazzeri, A. Vittadini, A. Selloni, Structure and energetics of stoichiometric TiO_2 anatase surfaces, Phys. Rev. B 63 (2001) 155409-1–155409-9.
[42] G.S. Herman, M.R. Sievers, Y. Gao, Structure determination of the two-domain (1 × 4) anatase TiO_2(001) surface, Phys. Rev. Lett. 84 (2000) 3354–3357.
[43] X.Q. Gong, A. Selloni, A. Vittadini, Density functional theory study of formic acid adsorption on anatase TiO_2(001): geometries, energetic, and effects of coverage, hydration, and reconstruction, J. Phys. Chem. B 110 (2006) 2804–2811.
[44] H.G. Yang, C.H. Sun, S.Z. Qiao, J. Zou, G. Liu, S.C. Smith, H.M. Cheng, G.Q. Lu, Anatase TiO_2 single crystals with a large percentage of reactive facets, Nature 453 (2008) 638–641.
[45] W. Zeng, T.M. Liu, Z.C. Wang, S. Tsukimoto, M. Saito, Y. Ikuhara, Oxygen adsorption on anatase TiO_2 (101) and (001) surfaces from first principles, Mater. Trans. 51 (2010) 171–175.
[46] Y. Han, C.J. Liu, Q.F. Ge, Effect of Pt clusters on methanol adsorption and dissociation over perfect and defective anatase TiO_2(101) surface, J. Phys. Chem. C 113 (2009) 20674–20682.
[47] A.M. Nadeem, G.I.N. Waterhouse, H. Idriss, The reactions of ethanol on TiO_2 and Au/TiO_2 anatase catalysts, Catal. Today 182 (2012) 16–24.
[48] L. Song, Y. Zhang, X. Wu, Z.G. Liao, Q.F. Yue, F.Y. Qu, X. Zhang, One-step synthesis of crystalline anatase TiO_2 nanospindles and investigation on their photocatalytic performance, Mater. Lett. 100 (2013) 198–200.
[49] J. Scaranto, S. Giorgianni, A DFT study of CO adsorbed on the clean and hydroxylated anatase TiO_2 (001) surfaces, Mol. Phys. 107 (2009) 1997–2003.
[50] B. Delley, An all-electron numerical method for solving the local density functional for polyatomic molecules, J. Chem. Phys. 92 (1990) 508–517.
[51] B. Delley, From molecules to solids with the $DMol^3$ approach, J. Chem. Phys. 113 (2000) 7756–7764.
[52] J.P. Perdew, K. Burke, M. Ernzerhof, Generalized gradient approximation made simple, Phys. Rev. Lett. 77 (1996) 3865–3868.
[53] J.P. Perdew, Y. Wang, Accurate and simple analytic representation of the electron-gas correlation energy, Phys. Rev. B 45 (1992) 13244–13249.
[54] P.J.D. Lindan, N.M. Harrison, M.J. Gillan, J.A. White, First-principles spin-polarized calculations on the reduced and reconstructed TiO_2(110) surface, Phys. Rev. B 55 (1997) 15919–15927.
[55] M. Dolg, U. Wedig, H. Stoll, H. Preuss, Energy-adjusted Ab initio pseudopotentials for the first row transition elements, J. Chem. Phys. 86 (1987) 866–872.
[56] A. Bergner, M. Dolg, W. Kuechle, H. Stoll, H. Preuss, Ab initio energy-adjusted pseudopotentials for elements of groups 13-17, Mol. Phys. 80 (1993) 1431–1441.
[57] P. Hohenberg, W. Kohn, Inhomogeneous electron gas, Phys. Rev. B 136 (1964) B864–B871.
[58] T.A. Halgren, W.N. Lipscomb, The synchronous-transit method for determining reaction pathways and locating molecular transition states, Phys. Rev. Lett. 49 (1977) 225–232.
[59] Y. Wang, H.J. Sun, S.J. Tan, H. Feng, Z.W. Cheng, J. Zhao, A.D. Zhao, B. Wang, Y. Luo, J.L. Yang, J.G. Hou, Role of point defects on the reactivity of reconstructed anatase titanium dioxide (001) surface [J], Nat. Commun. 4 (2013) 2214-1–2214-8.